PII: S0032-3861(97)10019-2

Polymer Vol. 39 No. 14, pp. 3135–3141, 1998

0032-3861/98/$19.00+0.00

Elongational flow-induced crystallization of poly(ethylene terephthalate) under the supercooled state†

Masami Okamoto, Hiroshi Kubo and Tadao Kotaka*
Advanced Polymeric Materials Engineering, Graduate School of Engineering, Toyota Technological Institute, Hisakata 2-12-1, Tempaku, Nagoya 468, Japan
(Received 5 June 1997; revised 18 July 1997; accepted 11 August 1997)

Elongational flow-induced crystallization in supercooled liquid poly(ethylene terephthalate) (PET) was investigated via elongational flow opto-rheometry (e.f.o.r.) and temperature-modulated differential scanning calorimetry (t.m.d.s.c.) in the temperature range 100–130°C, in which the blow moulding operation on PET is usually conducted. Measurements of tensile stress $\sigma(t)$ and birefringence $\Delta n(t)$ as a function of the Hencky strain rate $\dot{\epsilon}_0$ and time t with e.f.o.r. revealed the features of their time evolution as being due to spherulite and/or flow-induced oriented crystalline formation during the elongation process. Below 110°C, where spherulite growth was negligible, elongational viscosity $\eta_E(t)$ ($=\sigma(t)/\dot{\epsilon}_0$) determined at different $\dot{\epsilon}_0$ first developed slowly and exhibited 'up-rising' or 'hardening' after certain periods of time $t_{\eta E}$; this behaviour reduced to a characteristic Hencky strain $\epsilon_{\eta E}$ ($=\dot{\epsilon}_0 t_{\eta E}$) $\cong 1.0$, independent of $\dot{\epsilon}_0$, reflecting the formation of flow-induced oriented crystallites beyond $\epsilon_{\eta E}$. At higher temperatures (~120–130°C), however, where spherulites that contributed significantly to η_E but little to $\Delta n(t)$ were formed during the resting period and/or in the early stage of elongation, the critical up-rising strain $\epsilon_{\eta E}$ varied from $\epsilon_{\eta E} \cong 0.5$ to $\epsilon_{\eta E} \cong 1.0$ as $\dot{\epsilon}_0$ was increased. Eventually the spherulites appeared to be deformed or broken down to form oriented crystallites. Analyses via t.m.d.s.c. combined with e.f.o.r. identified spherulites in the specimens elongated at high temperatures but flow-induced oriented crystallites in those elongated at low temperatures. © 1998 Elsevier Science Ltd. All rights reserved.

(Keywords: elongation; flow-induced crystallization; poly(ethylene terephthalate))

INTRODUCTION

Elongation of molten polymers is one of the most important deformation patterns in various polymer processing operations such as fibre spinning, film blowing and blow moulding[1–8]. Understanding of the elongational flow behaviour may lead to optimization of these processing conditions. In the blow moulding process for semicrystalline polymers such as poly(ethylene terephthalate) (PET) under the supercooled state, one often encounters a difficulty of so-called 'whitening' induced by crystallization in the liquid during the blow moulding process and/or afterwards in the annealing stage of the product. To avoid this difficulty, we need to understand elongational-flow-induced orientation, anisotropy and crystallization behaviour of semicrystalline polymers in the supercooled state.

Polymer melt elongation has been extensively studied and its features have been clarified, especially by Meissner and his colleagues with an elongational rheometer of the rotary clamp/liquid supporting type[9] and more recently with a more sophisticated version of the metal conveyer belt/gas cushion type[10] commercialized as Rheometrics Melts Elongational Rheometer (RME). On the other hand, to study flow-induced orientation and deformation of polymer chains in the molten state, flow birefringence is a promising technique[11–14]. In fact, flow birefringence data were accumulated and the well-known linear stress–optical law was claimed to be proven as valid for molten polymers under shear flow, even in the nonlinear region where a tendency towards shear thinning was prevailing[13–15].

In an earlier attempt to understand the structural formation in crystalline polymers during melt elongation, Katayama *et al.* examined the isothermal melt spinning process of some polyolefines by observing the birefringence and flow properties along the spinline in order to correlate molecular orientation and crystallization under the melt spinning conditions[16]. Elongational flow-induced crystallization in supercooled polypropylene was discussed by Koyama *et al*[17] who were, however, concerned mainly with elongational viscosity data but not with the observation of the structure formation process during elongation.

The necessity of combining elongational flow rheometry and the flow birefringence technique was obvious. We thus attempted and successfully completed the installation into Meissner's new elongational rheometer[10], taking advantage of its new features, of a high precision birefringence apparatus to look into the internal structure of polymer melts under elongation[18]. We tentatively called the system 'elongational flow opto-rheometer (e.f.o.r.)'; it enabled us to make simultaneous measurements of transient tensile stress and birefringence as a function of time under a constant (Hencky) strain rate from 0.001 to 1.0 s^{-1} up to the maximum Hencky strain of as much as 7 that was covered by the RME[10].

With this e.f.o.r. we pursued the solution of several problems involved in the proccessing operations of supercooled crystalline polymer liquids such as poly(ethylene

* To whom correspondence should be addressed
† Elongational flow opto-rheometry for polymeric liquids, Part 2

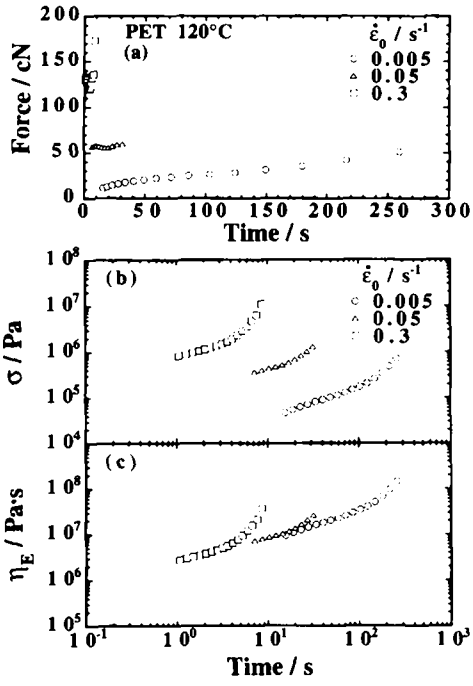

Figure 1 (a) Tensile force *versus* time t, (b) double logarithmic plots of tensile stress σ *versus* t and (c) of elongational viscosity $\eta_E(t) = \sigma/\dot{\epsilon}_0$, for PET elongated at 120°C with various strain rates $\dot{\epsilon}_0$ as indicated

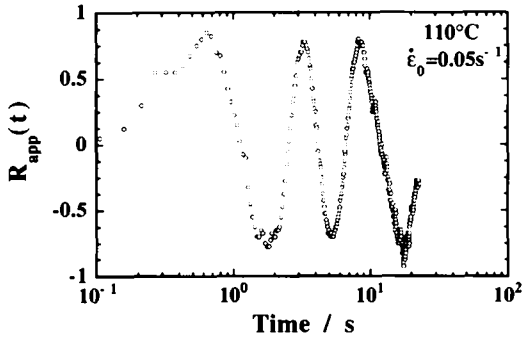

Figure 2 Time evolution of the apparent retardation, $R_{app}(t)$, in e.f.o.r. run for PET elongated at 110°C with a strain rate of $\dot{\epsilon}_0 = 0.05\ s^{-1}$

terephthalate) (PET) and revealed the features of elongational flow-induced crystallization behaviour. To our knowledge, there have been no such studies reported so far which clearly demonstrate elongational flow-induced crystallization, although there a large number of studies are available on shear-induced and/or strain-induced crystallization[19–25]. As is well known, PET enjoys wide application for the production of fibres, films and beverage bottles. However, there are still many unsolved issues concerning its orientational crystallization behaviour under elongational flow as occurs in blow moulding processes. Thus this study may hopefully contribute towards clarifying the problems of structure development during these processes.

EXPERIMENTAL

Polymer sample

A commercial poly(ethylene terephthalate) (PET) sample of blow-moulding grade was supplied by Toyobo Co. The glass transition and melting temperatures were $T_g = 76$°C and $T_m = 253$°C, respectively. The weight-average molecular weight M_w was 54×10^3, the polydispersity index $M_w/M_n = 2.2$ and the intrinsic viscosity (η) was 0.79 (dl g^{-1}) in a mixture of *p*-chlorophenol and 1,1,2,2-tetrachloroethane (3:1 v/v) at 30°C. PET pellets were dried under a reduced pressure of 10^{-4} torr at 140°C for 16 h to remove water before being subjected to compression moulding. The pellets were sandwiched between polyimide films (Kapton® HN, Toray–DuPont) and compression moulded with a laboratory hot press kept at 290°C ($> T_m$ of PET) for 90 s. The moulded sheet was quickly quenched to room temperature by sandwiching it with glass plates to obtain an amorphous sheet, which was then cut into thin strips of 60 mm × 7 mm × 0.4 mm in size and later subjected to e.f.o.r. measurements.

Spherulite growth under a quiescent state

We also observed spherulite growth behaviour of PET under a quiescent state in the temperature range between 110 and 130°C to see the effect of crystallization on the elongational flow behaviour. Dried pellets were sandwiched between two pieces of cover glass, placed in a laboratory hot press and compression moulded at 290°C for 90 s to obtain a thin film of ~30 μm thickness. Then the molten film was rapidly quenched to the desired supercooled state between 110 and 130°C by putting it on a thermostatted hot-stage (Linkam LK600PM, Linkam Scientific Instruments Ltd) mounted on a polarizing optical microscope (Nikon OPTIPHOTO2-POL). The variation with time of the radii of the PET spherulites was then observed with the microscope equipped with a photographic film recording system.

Shear viscosity

Dynamic viscoelastisic and zero shear viscosity η measurements were carried out on a Rheometrics Dynamic Analyzer (RDAII) with a cone-plate geometry having a cone angle of 0.1 rad and a diameter of 25 mm. First we attempted to determine the shear viscosity in the temperature range 100–150°C covered in the elongation experiments. It turned out that, at these temperatures, the PET specimen did not adhere to the surfaces of the cone and plate and thus slipped between the gap. We therefore raised the temperature to the range of 260–290°C ($> T_m$ of PET) and conducted the dynamic viscosity and time development of steady shear viscosity measurements under a nitrogen atmosphere. In the former study the strain amplitude imposed was kept less than 5%, which was in the range of linear viscoelasticity. In the latter, a typical shear rate was $\dot{\gamma} \cong 0.05\ s^{-1}$ at which molten PET exhibited Newtonian behaviour. The steady shear viscosities η in the 100–150°C range were estimated by using the universal Williams–Landel–Ferry (WLF) equation[26] and/or Arrhenius fit. We expected that the values of η thus estimated correspond to those of a hypothetical supercooled liquid state of PET in which no crystallites exist.

E.f.o.r. tests

In the e.f.o.r. run, an amorphous strip was placed in the sample supporting system, set at a desired crystallization temperature between 100 and 130°C and annealed for 90 s before starting the measurement[10,18]. The details are described elsewhere[18]. *Figure 1* shows examples of time evolution of (a) tensile force, (b) tensile stress and (c) elongational viscosity obtained on PET at 120°C. In contrast, *Figure 2* shows an example obtained at 110°C for the apparent retardation $R_{app}(t) \propto \sin(2\Delta)$, Δ being the

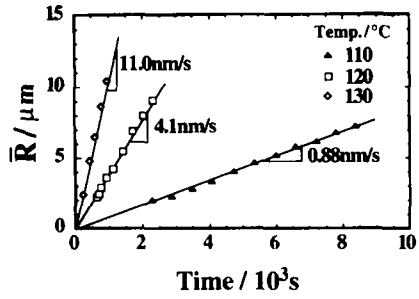

Figure 3 Time variation of the radii of PET spherulites under quiescent state during isothermal crystallization at various temperatures between 110 and 130°C

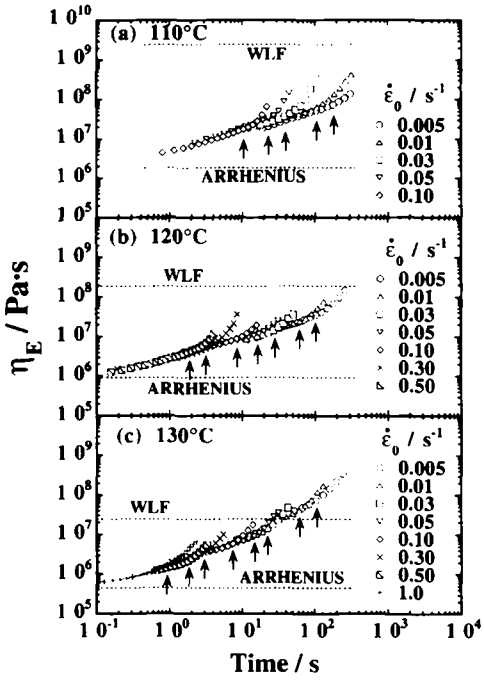

Figure 4 Time variation of elongational viscosity $\eta_E(t)$ in various supercooled states with various $\dot{\epsilon}_0$ from 0.005 to 1.0 s^{-1}. The dotted lines marked as WLF or Arrhenius are 3 times zero-shear viscosity, $3 \times \eta_0$, extrapolated by using either WLF fit or Arrhenius plot from high temperature (260-290°C > $T_m \approx$ 253°C) shear viscosity values. The arrows indicate up-rising time $t_{\eta E}$ at which $\eta_E(t)$ begins to deviate from the linear ($\dot{\epsilon}_0$-independent) $\eta_E(t)$ *versus* t curve

phase difference from which the birefringence $\Delta n(t)$ was calculated[18].

T.m.d.s.c. analysis

To estimate the degree of crystallinity of the elongated specimens, we carried out temperature modulated differential scanning calorimetry (t.m.d.s.c.) using an MDSC™ (TA 2920, TA Instruments). T.m.d.s.c. is a new technique[27] in which a test specimen is subjected to a modulated heating mode composed of a sinusoidal temperature variation of amplitude ΔT and frequency ω superposed on a linear heating mode with constant heating rate. Deconvolution of the resulting net heat flow profile provides the total heat flow obtained from conventional d.s.c., but also separates it into heat capacity-related (reversing) and kinetics-related (non-reversing) components; an example of the thermogram is shown later in *Figure 7*. T.m.d.s.c. is a powerful tool to determine the true initial degrees of crystallinity unobscured by crystallization/remelting which often takes place during the heating process in conventional d.s.c.[28].

For the combined e.f.o.r.–t.m.d.s.c. analysis, a test specimen subjected to e.f.o.r. to a certain extent of elongation was quickly quenched by sandwiching it between cold metal plates to freeze the internal structure developed during the elongation. A sample weighing approximately 10 mg was cut out from the centre of the quenched specimen and subjected to the t.m.d.s.c. test. In such a test, usually a heating/cooling cycle of modulation period 60 s and amplitude ± 0.5°C was superposed on a steady heat flow of + 10°C min^{-1} rate under a nitrogen stream.

RESULTS

Spherulite growth

In order to analyse elongational flow-induced crystallization, first we need to know the isothermal crystallization behaviour of PET under a quiescent state. *Figure 3* shows time t variation of the spherulite radii $\bar{R}$ at various supercooled states. A linear increase in $\bar{R}$ passing through the origin is seen over a wide range of the time scale, implying that the volume fraction increases in proportion to t^3. Note that spherulite growth occurs immediately after the temperature drop, with zero induction time. This fact suggests that heterogeneous nucleation occurs[29,30]. Within the range of 110–130°C examined the growth rate, defined as the initial slope of the $\bar{R}$ *versus* t relation (= $d\bar{R}/dt$), increases with increasing crystallization temperature. At 130°C the rate is as much as 10 times faster than that at 110°C.

Elongational viscosity

Figure 4 shows some examples of time t variation of elongational viscosity $\eta_E(t)$ taken at various strain rates $\dot{\epsilon}_0$ at three different temperatures. In each figure the dotted lines marked as $3\eta_0$ indicate three times the shear viscosity η_0 for the hypothetical supercooled state estimated from the high-temperature shear-viscosity value by using the universal WLF equation[26], because we were unable to determine directly the development of shear viscosity $\eta(t)$ at these temperatures. We also estimated $3\eta_0$ using an Arrhenius-type equation defined by:

$$\ln a_T \equiv \ln \frac{\eta_T}{\eta_{T_0}} = \frac{\Delta H^*}{R}\left(\frac{1}{T} - \frac{1}{T_0}\right) \qquad (1)$$

where η_T and η_{T_0} are the zero shear viscosities at T and T_0, respectively, ΔH^* the apparent activation enthalpy for viscous flow, R the gas constant and T_0 a reference temperature.

We first determined $\Delta H^* = 94$ kJ mol^{-1} from dynamic viscoelasticity and steady shear viscosity data in the temperature range 260–290°C. Then we determined the shift factor a_T and estimated the zero shear viscosity η_T at a temperature T in the range of 100–150°C. The estimated $3\eta_0$ (= $3\eta_T$) values are shown in each figure by dotted lines marked either as 'WLF' or as 'Arrhenius'. The levels of $3\eta_0$ marked as WLF are apparently too high, while those marked as Arrhenius appear to be reasonable or can be a little too low.

For all these cases $\eta_E(t)$ starts from a relatively high level in the very beginning, gradually increases with t without showing dependence on $\dot{\epsilon}_0$, and then the curves begin to diverge from each other at a certain 'up-rising' time $t_{\eta E}$

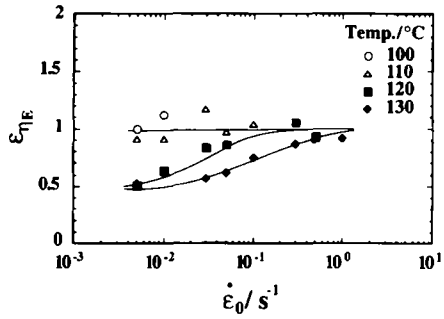

Figure 5 Strain rate $\dot{\epsilon}_0$-dependence of up-rising Hencky strain $\epsilon_{\eta E}$(= $\dot{\epsilon}_0 \cdot t_{\eta E}$) in various supercooled states between 100 and 130°C

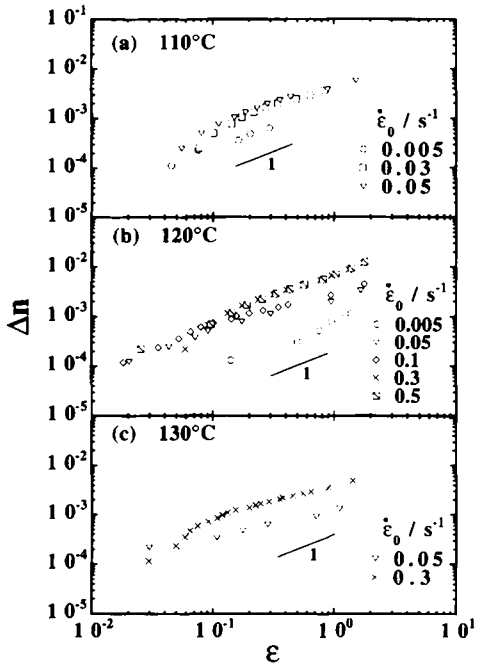

Figure 6 Double logarithmic plots of birefringence $\Delta n(t)$ *versus* Hencky strain ϵ (= $\dot{\epsilon}_0 t$). The solid lines indicate a slope of 1

dependent on $\dot{\epsilon}_0$ in such a way that $t_{\eta E}$ becomes shorter with increasing $\dot{\epsilon}_0$, as shown in *Figure 4* by the upward arrows. After $t_{\eta E}$, $\eta_E(t)$ increases with t more rapidly.

In the case of amorphous polymer liquids such as polystyrene (PS), or crystalline polymer melts such as low density polyethylene (LDPE), their $\eta_E(t)$ *versus* t profiles exhibit several common features[18]. One is that the common portion of the $\eta_E(t)$ *versus* t curves usually has an upward convex curvature and does obey, below certain $t_{\eta E}$, the linear viscoelasticity rule which states that $\eta_E(t) = 3\eta(t)$, as found in other molten polymers‡[9,18]. The other is that the $\eta_E(t)$ *versus* t curves then exhibit more or less a tendency of 'strain hardening' with a downward convex curvature after $t_{\eta E}$ (that is nearly an inflection point), dependent on $\dot{\epsilon}_0$ in such a way that the up-rising Hencky strain $\epsilon_{\eta E} = \dot{\epsilon}_0 \cdot t_{\eta E}$ is nearly constant, independent of $\dot{\epsilon}_0$[1-8].

As for the first feature, because we were unable to determine $3\eta(t)$ for supercooled PET liquids we cannot tell for sure whether or not the linear viscoelasticity rule was also obeyed‡. Nevertheless, a common portion of the $\eta_E(t)$ *versus* t curves exists and that portion may be regarded as 'linear' in the sense that $\eta_E(t)$ is independent of $\dot{\epsilon}_0$, while the up-rising portion after $t_{\eta E}$ can be regarded as 'nonlinear' in the opposite sense.

The shape of the $\eta_E(t)$ *versus* t curves of the PET liquids is different from those for PS and LDPE melts, and the curves obtained at 110°C and 130°C also differ from each other. For the PET liquids, on both sides of $t_{\eta E}$, the curve increases with t more or less with a downward convex curvature; that is, the $t_{\eta E}$ is not an inflection point. Then, looking at the curves more closely, we notice that at 110°C the linear portion of the curves increases with t rather slowly but the nonlinear portion rather rapidly, while at 130°C the tendency is opposite so that the $\eta_E(t)$ *versus* t curves exhibit more gradual change than those at 110°C.

To see whether or not the feature that the up-rising of $\eta_E(t)$ takes place at a common up-rising Hencky strain $\epsilon_{\eta E} = \dot{\epsilon}_0 \cdot t_{\eta E}$ ($\approx$ constant) for a melt elongated with different $\dot{\epsilon}_0$ is also the case for supercooled PET liquids, we plotted in *Figure 5* the $\dot{\epsilon}_0$-dependence of $\epsilon_{\eta E}$ at various temperatures, and found that they show somewhat different behaviour from that of PS and LDPE melts. Note in *Figure 5* that, for example, at 130°C with lower $\dot{\epsilon}_0$ ($< 0.05\ s^{-1}$), $\epsilon_{\eta E}$ remains at the level of 0.5 to 0.6 and gradually increases to the level of 1.0 as $\dot{\epsilon}_0$ is increased beyond $0.05\ s^{-1}$. On the other hand, at 100 or 110°C, $\epsilon_{\eta E}$ remains almost constant, around 1.0, over the whole range of $\dot{\epsilon}_0$ covered in these experiments.

Birefringence

Figure 6 summarizes birefringence $\Delta n(t)$ *versus* Hencky strain ϵ (= $\dot{\epsilon}_0 t$) curves with varying $\dot{\epsilon}_0$ from 0.005 to $0.5\ s^{-1}$ obtained at three different temperatures as indicated. For PS and LDPE melts, the $\Delta n(\epsilon)$ as well as the tensile stress $\sigma(\epsilon)$ *versus* ϵ curves exhibited strong $\dot{\epsilon}_0$-dependence[18]. We also observed, for PET, $\dot{\epsilon}_0$-dependent $\Delta n(\epsilon)$ *versus* ϵ profiles but in a somewhat different manner. Note that the tendency of upward deviation of $\Delta n(\epsilon)$ *versus* ϵ curves after $\epsilon_{\eta E}$ (which has often been observed in PS and LDPE melts[18]) is not observed for the supercooled PET liquids at any temperatures or strain rates $\dot{\epsilon}_0$. At 110°C each curve is a straight line with a slope of approximately 1, while at higher temperatures the slope reduces to around 0.67, as seen in *Figure 6*. This implies that the $\Delta n(\epsilon)$ *versus* ϵ profiles related to flow-induced segment orientation behaviour are different at different temperatures, for which the difference in spherulite growth mode in PET is presumably responsible.

DISCUSSION

Effect of crystallization

The time evolution of $\sigma(t)$ and $\Delta n(t)$ *versus* ϵ(= $\dot{\epsilon}_0 t$) profiles suggests that crystalline formation, or more precisely spherulite formation and/or oriented crystallite formation, is playing a crucial role in the elongation of supercooled PET liquids. The spherulite growth behaviour shown in *Figure 3* suggests the following. In the e.f.o.r. run at 110°C hardly any spherulite growth takes place during the initial 90 s annealing time, while in the later stages flow-induced oriented crystallite formation may take place. On the other hand, at 130°C considerably large spherulites of radius $\bar{R}$ as large as 1 μm may be formed and the existing spherulites may increase the stresses in the early stage of elongation, while in the intermediate-to-later stages the spherulites may grow, to be deformed or even reorganized

‡ Our recent results on narrow MWD, high molecular weight PS suggest that this is not always the case: in such a melt, $3\eta(t)$ was found to be smaller than $\eta_E(t)$ by a factor of 5–30%.

into flow-induced oriented crystallites. However, in e.f.o.r. a tough sample with a high degree of crystallinity often slips between the metal belt cramps when stretched, especially at high $\dot{\epsilon}_0$. This makes it difficult to maintain the transient stress and birefringence measurements up to large ϵ (see *Figure 1*).

To examine the effects of crystallization, we recovered a small portion from the centre of PET specimens elongated with $\dot{\epsilon}_0 = 0.01\ s^{-1}$ at 110 and 130°C to various extents of ϵ, and subjected them to t.m.d.s.c. analysis according to the method described in the EXPERIMENTAL section. *Figure 7* is just one example of a t.m.d.s.c. scan of a PET sample elongated up to $\epsilon = 1.75$ in Hencky units with $\dot{\epsilon}_0 = 0.01\ s^{-1}$ at 110°C, showing (a) the total heat flow, (b) the reversing and (c) nonreversing heat flows. The total heat flow is the sum of the reversing (the in-phase component in ΔT-modulation) and the nonreversing signals.

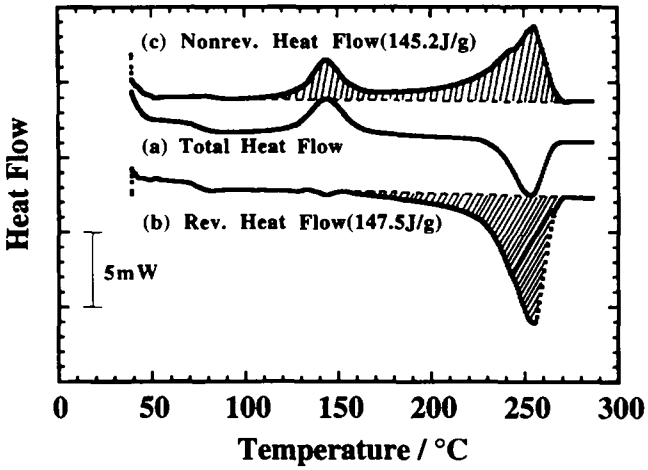

Figure 7 T.m.d.s.c. scan for a specimen elongated up to $\epsilon = 1.75$ with $\dot{\epsilon}_0 = 0.01 s^{-1}$ at 110°C: (a) total flow; (b) reversing heat flow; and (c) nonreversing heat flow

In a conventional d.s.c. run on a quenched crystalline polymer specimen, one often sees that additional crystallization takes place during the heating process of the run. Thus, to estimate the true degree of crystallinity χ_c present in the sample before being subjected to the d.s.c. test, we have to subtract the extra heat due to the crystallites formed during the heating process from the total endothermic heat flow of the crystalline melting. On the t.m.d.s.c. run the endothermic heat flow ΔH_{diff} from the initially existing crystallites can be easily calculated as $\Delta H_{diff} = \Delta H_{rev} - \Delta H_{nonrev}$, where ΔH_{rev} is the endothermic melting (reversing) enthalpy from the reversing heat flow profile and ΔH_{nonrev} is the exothermic ordering/crystallization (nonreversing) enthalpy from the nonreversing heat flow profile appearing in the temperature range 100–290°C as seen in *Figure 7*. In this particular run, the enthalpies were $\Delta H_{rev} = 147.5\ J\ g^{-1}$ and $\Delta H_{nonrev} = 145.2\ J\ g^{-1}$. The χ_c was thus calculated as $\chi_c = \Delta H_{diff}/\Delta H^0 = 1.9 \pm 1.1\%$, with $\Delta H^0 = 122\ J\ g^{-1}$ being the melting enthalpy of 100% crystalline PET[31].

Figure 8 summarizes the results for specimens elongated with $\dot{\epsilon}_0 = 0.01\ s^{-1}$ at 110°C (triangles) and at 130°C (squares): (a) the cold crystallization temperature T_{cc}

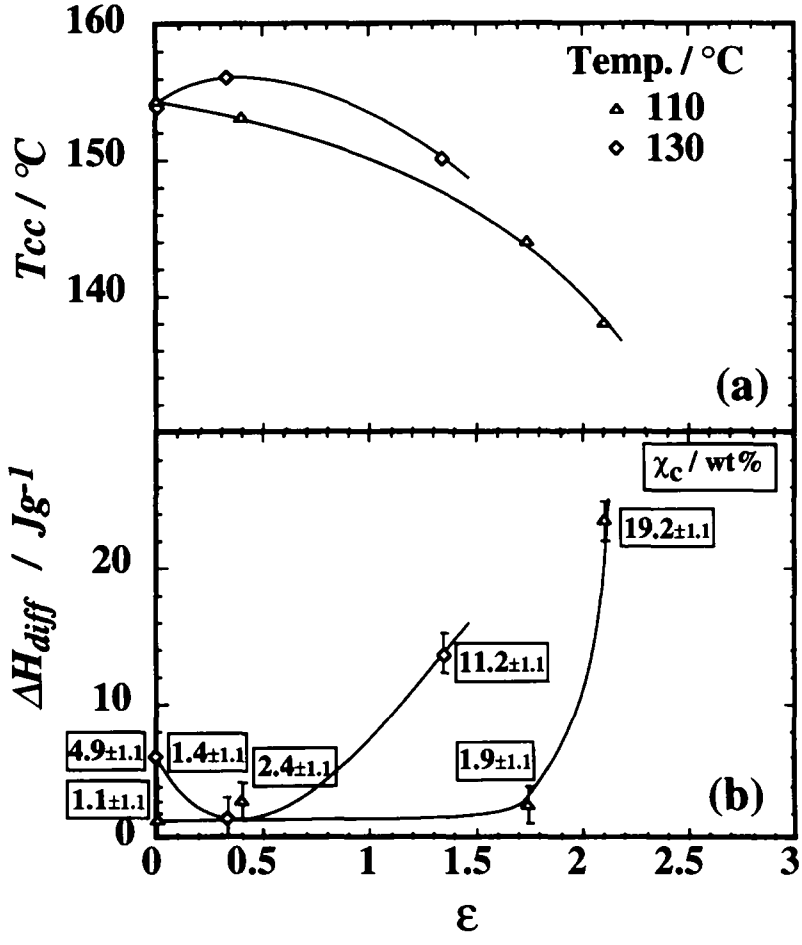

Figure 8 Plots of (a) cold crystallization temperature T_{cc} and (b) difference of the heat flow ΔH_{diff} for PET elongated with $\dot{\epsilon}_0 = 0.01\ s^{-1}$ at 110 (triangles) and 130°C (squares). The degree of %-crystallinity χ_c of each specimen is shown by the number in the box

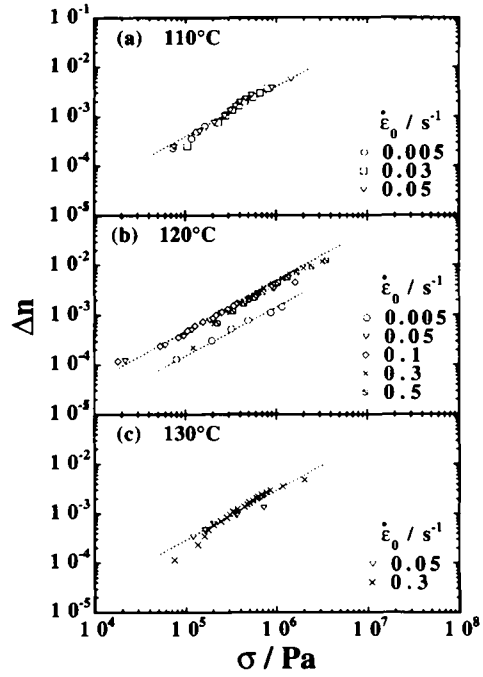

Figure 9 Double logarithmic plots of birefringence $\Delta n(t)$ *versus* tensile stress $\sigma(t)$ elongated with constant strain rates $\dot{\epsilon}_0$ at various temperatures: (a) 110°C; (b) 120°C; and (c) 130°C. The dashed lines indicate the slope 1

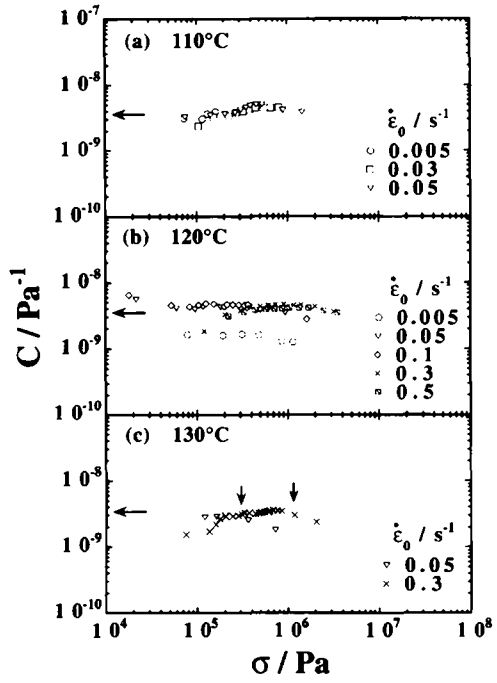

Figure 10 Double logarithmic plots of $C(=\Delta n/\sigma)$ *versus* $\sigma(t)$ for the specimens elongated with constant strain rates $\dot{\epsilon}_0$ as indicated at various temperatures: (a) 110°C; (b) 120°C; and (c) 130°C. The arrows pointing to the C-axis indicate the reported value of C ($\cong 3.56 \times 10^{-9}$ Pa^{-1}), whereas those attached to the two curves in the panel (c) indicate the stress corresponding to their up-rising Hencky strains $\epsilon_{\eta E}$

(determined as the exothermic peak temperature appearing on the lower temperature side of the nonreversing heat flow profile) and (b) $\Delta H_{\text{diff}} = \Delta H_{\text{rev}} - \Delta H_{\text{nonrev}}$ and the true degrees of crystallinity χ_c thus calculated (the numbers in the box attached to the symbols).

At 130°C spherulite formation is dominant, whereas at 110°C elongational flow-induced (orientational) crystallization seems to prevail. For the specimens elongated at 130°C, the T_{cc} first slightly increases and then decreases, whereas for those at 110°C the T_{cc} constantly decreases with increasing ϵ compared with those crystallized in the quiescent state (see *Figure 8a*). The lower T_{cc} value for those elongated at 110°C than at 130°C suggests that the specimens elongated at lower temperatures and quenched are more easily crystallizable during the d.s.c. heating process. In *Figure 8b*, we see that for the specimens elongated at 110°C the ΔH_{diff} at the onset of elongation are very small (thus $\chi_c \cong 0$) and remain small until ϵ reaches 1.75 in Hencky units ($\cong \epsilon_{\Delta n}$), beyond which they increase rapidly to reach $\chi_c \cong 19.2$ wt% at $\epsilon \approx 2.1$. On the other hand, at 130°C, the ΔH_{diff} is 6 J g^{-1}, corresponding to $\chi_c \cong 4.9\%$ crystallinity at $\epsilon = 0$ (due to spherulite formation before stretching), attains a minimum at $\epsilon \approx 0.4$ and then increases again to reach $\chi_c \cong 11.2\%$ at $\epsilon \approx 1.35$, beyond which the strip begins to slip. Our unpublished Rayleigh scattering studies reveal that the morphology of the crystallites with $\chi_c = 11.2\%$ at 130°C is deformed spherulites, whereas that with $\chi_c \cong 19.2\%$ at 110°C is oriented crystallites of shish-kebab type[32].

These results suggest that at 130°C the onset of elongation deformed once-developed spherulites during the rest period and reduced the degree of crystallinity. However, the polymer's basically spherulite-forming nature surpasses the destruction of the initially existing spherulites so that, if $\dot{\epsilon}_0$ is not too high, new spherulites are continuously created and deformed in the later stages, accompanying a gradual increase in ΔH_{diff} with increasing ϵ. On the other hand, at 110°C, initially no spherulites do exist but, after $\epsilon \approx 2(\cong \epsilon_{\Delta n})$, flow-induced oriented-crystalline formation with shish-kebab morphology proceeds and χ_c becomes as large as 19.2 wt%. This behaviour reasonably well explains the tendency of upward deviations of η_E at the different supercooled states, because spherulites may contribute to the tensile stresses but may not contribute to the birefringence. These features are probably common in the elongation of supercooled liquids of crystalline polymers.

The stress optical rule

It has been believed that the stress optical rule holds for the deformation of rubbers[33] and for the more general problem of polymeric liquid rheology as well, because both the stress and the birefringence have the same physical origin, that is, the orientational ordering in the polymer segments[15]. The stress optical rule states that a simple proportionality exists between the refractive index and the deviatric (anisotropic) stress tensors. Thus, for polymer melt elongation, the rule reads:

$$\Delta n(t) = C(t)\sigma(t) \tag{2}$$

where $C(t)$, the stress optical coefficient first given by Treloar *et al.*[33,34] for rubber elasticity, is supposed to be independent not only of ϵ or σ but also of $\dot{\epsilon}_0$ if the stress optical rule strictly holds. So far the values of C have been determined mostly from shear flow experiments on varieties of polymer melts[13-15,34-36].

In our e.f.o.r. experiments on supercooled PET liquids, the stress optical rule may have been violated because creation of spherulites and/or formation of oriented crystallites took place during the elongation. *Figure 9* shows replots of the data shown in *Figures 4, and 6* in the double logarithmic form of $\Delta n(t)$ *versus* tensile stress $\sigma(t)$. In *Figure 10* these data are again replotted in the double logarithmic form of stress optical coefficient $C(t)$ *versus* $\sigma(t)$.

The relations between C and σ shown in *Figure 10* are almost independent of $\dot{\epsilon}_0$, and the values of C are the same as those determined from dynamic shear flow experiments[37]. At 130°C we see a slightly downward deviation of the $C(t)$ *versus* $\sigma(t)$ curves beyond $\epsilon_{\eta E}$, where σ further increases but $\Delta n(t)$ remains practically unchanged due presumably to the influence of spherulite formation. At 120°C, with low $\dot{\epsilon}_0 (= 0.005 s^{-1})$, the value of C is smaller than the reported value. The downward deviation of $C(t)$ *versus* $\sigma(t)$ relations under large $\dot{\epsilon}_0$ was not observed in noncrystalline, amorphous polymer melts[18]. These contrasts between the supercooled PET liquids and other amorphous polymer melts imply that tensile stress relaxation may hardly occur under the formation of spherulites. These results reflect complex influences of crystallization and may be common in the elongation of supercooled liquids of crystalline polymers.

CONCLUSION

With e.f.o.r. we have demonstrated complicated processes in the elongational flow behaviour of PET in the supercooled states. In the low temperature region ($\approx$ 100–110°C), where spherulite formation is negligible, the effect of crystallization on the 'up-rising' in η_E is rather small, so that $\epsilon_{\eta E}$ remains almost constant (~ 1) regardless of $\dot{\epsilon}_0$. Elongational flow-induced crystallization may follow beyond $\epsilon_{\Delta n} \approx 2 (> \epsilon_{\eta E})$, as revealed by t.m.d.s.c. analysis. In high temperature ($\approx$120–130°C) elongation, however, spherulite growth may take place so that $\epsilon_{\eta E} (< 1)$ is small, especially in low $\dot{\epsilon}_0$ elongation, whereas in high $\dot{\epsilon}_0$ elongation $\epsilon_{\eta E}$ becomes constant, reflecting that deformation of the grown spherulites is under way.

The spherulites formed in PET at 130°C may contribute to the enhancement of tensile stress but may hamper the elongational flow-induced orientation. The effect of crystallization prevailing, especially in the high σ (or ϵ) region, may lead to enhancement in σ larger than that expected from the elastic stress contribution[15], reducing C to beyond $\epsilon_{\eta E}$. At high temperatures the complex features involving spherulite formation before elongation, subsequent spherulite deformation/breakdown and reorganization into flow-induced oriented crystallites may be responsible for the elongational flow behaviour of supercooled PET liquids.

REFERENCES

1. Cogswell, F. N., *Trans. Soc. Rheol.*, 1972, **16**, 383.
2. Meissner, J., *Pure Appl. Chem.*, 1975, **42**, 553.
3. Ide, Y. and White, J. L., *J. Appl. Polym. Sci.*, 1978, **22**, 1061.
4. Pearson, G. H. and Connelly, R. W., *J. Appl. Polym. Sci.*, 1992, **27**, 969.
5. Kwack, T. H. and Han, C. D., *J. Appl. Polym. Sci.*, 1983, **28**, 3419.
6. Winter, H. H., *Pure Appl. Chem.*, 1983, **55**, 943.
7. Kanai, T. and White, J. L., *Polym. Eng. Sci.*, 1984, **24**, 1185.
8. Utracki, L. A. and Schlund, B., *Polym. Eng. Sci.*, 1987, **27**, 1512.
9. Meissner, J., *Rheol. Acta*, 1969, **8**, 78.
10. Meissner, J. and Hostettler, J., *Rheol. Acta*, 1994, **33**, 1.
11. Petrie C. J. S., *Elongational Flows*. Pitman, London, 1979.
12. Barnes, H. A., Hutton, J. F. and Walters, K., *An Introduction to Rheology*, Chapter 5. Elsevier, Amsterdam, 1989.
13. Janeschitz-Kriegel, H., *Adv. Polym. Sci.*, 1969, **6**, 170–318.
14. Janeschitz-Kriegl, H., *Polymer Melt Rheology and Flow Birefringence*. Springer-Verlag, Berlin, 1983.
15. Doi, M. and Edwards, S. F., *The Theory of Polymer Dynamics*. Clarendon Press, Oxford, 1986, pp. 221–222.
16. Katayama, K., Amano, T. and Nakamura, K., *Appl. Polym. Symp.*, 1973, **20**, 237.
17. Ito, H., Kawamura, T., Takimoto, J. and Koyama, K., *Seikeikakou*, 1995, **7**, 576.
18. Kotaka, T., Kojima, A. and Okamoto, M., *Rheol. Acta*, 1998, (in press).
19. Pennings, A. J., van der Mark, J. M. and Booij, H. C., *Kolloid Z. u Z. Polym.*, 1970, **236**, 99.
20. McHugh, A. J. J., *Appl. Polym. Sci.*, 1975, **19**, 125.
21. Stein, R. S., *Polym. Eng. Sci.*, 1976, **16**, 152.
22. Lagasse, R. R. and Maxwell, B., *Polym. Eng. Sci.*, 1976, **16**, 189.
23. Pennings, A. J., *J. Polym. Sci., Polym. Symp.*, 1977, **59**, 55.
24. Salem, D. R., *Polymer*, 1994, **35**, 771.
25. Ajji, A., Guevremont, J., Cole, K. C. and Dumoulin, M. M., *Polymer*, 1996, **37**, 3707.
26. Ferry, J. D., *Viscoelastic Properties of Polymers*, Chap. 11. John Wiley & Sons, New York, 1961.
27. Sauerbrunn, S. and Gill, P., *Am. Lab.*, 1993, **25**, 54.
28. Wunderlich, B., Jin, Y. and Boller, A., *Thermochim. Acta*, 1994, **238**, 277.
29. Lee, C. H., Saito, H. and Inoue, T., *Macromolecules*, 1993, **26**, 6566.
30. Lee, C. H., Saito, H., Inoue, T. and Nojima, S., *Macromolecules*, 1996, **29**, 7034.
31. Wunderlich, B., *Macromolecular Physics*, Vol. 3. Academic Press, New York, 1980.
32. Kubo, H., Sato, H., Okamoto, M. and Kotaka, T., *Polymer*, 1998, **39**, 501.
33. Treloar, L. R. G., in *Die Physik der Hochpolymeren*, ed. H. A. Stuart, Chap. 4. Springer-Verlag, Berlin, 1956.
34. Treloar, L. R. G., *The Physics of Rubber Elasticity*, 3rd edn. Clarendon Press, Oxford, 1975.
35. Gortemaker, F. H., Hansen, M. G., de Cindio, B., Laun, H. M. and Janeschitz-Kriegl, H., *Rheol. Acta*, 1976, **15**, 256.
36. Zebrowski, B. E. and Fuller, G. G., *J. Polym. Sci., Polym. Phys. Ed.*, 1981, **19**, 531.
37. Inoue, M. and Osaki, K., Abstract of the 8th Jpn Soc. Rheol. Symp. on Polymer Processing Technologies, Nagoya, 1996, pp. 59–60.